Utility of Ground-Penetrating Radar as a Root Biomass Survey Tool in Forest Systems

J. R. Butnor,* J. A. Doolittle, K. H. Johnsen, L. Samuelson, T. Stokes, and L. Kress

ABSTRACT

Traditional methods of measuring tree root biomass are labor intensive and destructive in nature. We studied the utility of ground-penetrating radar (GPR) to measure tree root biomass in situ within a replicated, intensive culture forestry experiment planted with loblolly pine (*Pinus taeda* L.). The study site was located in Decatur County, Georgia, in an area of the Troup and Lucy (loamy, kaolinitic, thermic Grossarenic Kandiudults and Arenic Kandiudults, respectively) soils. With the aid of a digital signal processing GPR, estimates of root biomass to a depth of 30 cm were correlated to harvested root samples using soil cores. Significant effects of fertilizer application on signal attenuation were observed and corrected. The correlation coefficient between actual root biomass in soil cores and GPR estimates with corrections for fertilizer application were highly significant ($r = 0.86$, $n = 60$, $p < 0.0001$). Where site conditions are favorable to radar investigation, GPR can be a powerful cost-effective tool to measure root biomass. Verification with some destructive harvesting is required since universal calibrations for root biomass are unlikely, even across similar soil types. Use of GPR can drastically reduce the number of soil cores needed to assess tree root biomass and biomass distribution. The quality and quantity of information resulting from a detailed GPR survey, combined with soil cores on a subset of plots, can be used to rapidly estimate root biomass and provide a valuable assessment of lateral root biomass distribution and quantity.

The contribution of tree roots to soil C is significant and difficult to survey accurately. In the southeastern USA, where excessive erosion from past farming practices has depleted the mineral soil of C, tree roots likely represent a greater proportion of belowground C. In a 34-yr-old loblolly pine ecosystem at the Calhoun Experimental Forest in Union County, South Carolina, root systems comprised 18% of the belowground C (Richter et al., 1995). At the Clemson Experimental Forest, in Oconee County, South Carolina, tree roots comprised 24% of the belowground C in a 55-yr-old loblolly pine plantation (Van Lear et al., 1995). Mineral soil C concentrations are very static in these established forest systems, Richter and others (1999) attributed <1% of current C sequestration to accretion in the mineral soil. Tree roots are the most dynamic pool for belowground C accumulation in these forests.

Traditional approaches used for root biomass harvests (e.g., soil cores, pits, and trenches) provide reasonably accurate information, but they are destructive in nature, labor intensive, and limited with respect to soil volume and surface area that can be assessed. Data derived from traditional root extraction approaches are also generally limited to root biomass averages across plots or treatments rather than information on root distribution. Sampling needed to detect differences among treatments can be expensive as well as time-consuming for technical personnel. Ground-penetrating radar can be used to detect tree roots and estimate root biomass rapidly and noninvasively (Butnor et al., 2001). While GPR may be an effective tool, its successful application is site specific. Ground-penetrating radar is limited by the electromagnetic properties of the soil being surveyed (Doolittle et al., 2002). Electrically resistive soils (i.e., high sand content) are more amenable to study then conductive soils. Site factors that limit detection of tree roots in the southeastern USA are considered in detail by Butnor et al. (2001). Without intensive, methodical scanning of grids, separation of roots by size class or depth is not practical (Butnor et al., 2001; Wielopolski et al., 2000).

Raw GPR data can be of great interpretive value to a trained technician in the field, but is typically used in a qualitative manner. Tasks such as mapping depth to bedrock or water table, estimating the dimensions of large subsurface objects, and delineating changes in soils are interpretable in the field. Quantitative analysis of raw data is possible. However, for the investigation of roots, soil features that are not the intended target often reduce the quality of the data. These undesired soil features produce clutter and interfere with data analysis. The goal of post-collection processing of radar data is to reduce clutter and minimize the effects of multiple hyperbolic reflections (Daniels, 1996). The radar image of a buried object often will not be representative of the objects' actual dimensions, and signal processing serves to transform the image to a format that can be more readily interpreted (Daniels, 1996). However, processing cannot replace the need for appropriate experimental design and amenable site conditions to gain meaningful root biomass data.

There are numerous factors that can interfere with the resolution of roots. This study explores the potential of GPR and processing techniques on a near-ideal site. The purpose of this research is to: (i) assess GPR as a rapid non-invasive means to augment destructive root biomass harvests, (ii) improve the quality of radar data through advanced processing techniques, (iii) calibrate/correlate radar estimates of root biomass with those obtained from soil cores, and (iv) determine if calibration is affected by block or treatment effects in a replicated study. The intent was to assess the full potential of GPR and processing techniques on a site that was, a priori, considered to be amenable to radar investigation.

J.R. Butnor, K.H. Johnsen, and L. Kress, Southern Research Station, USDA Forest Service, 3041 Cornwallis Road, Research Triangle Park, NC 27709; J.A. Doolittle USDA-NRCS, 11 Campus Boulevard, Suite 200 Newtown Square, PA 19073; L. Samuelson and T. Stokes, School of Forestry & Wildlife Sciences, Auburn Univ., Auburn, AL 36849. Received 7 Jan. 2002. *Corresponding author (jbutnor@fs.fed.us).

Published in Soil Sci. Soc. Am. J. 67:1607–1615 (2003).
© Soil Science Society of America
677 S. Segoe Rd., Madison, WI 53711 USA

Abbreviations: GPR, ground-penetrating radar; SIR, subsurface interface radar.

MATERIALS AND METHODS

Study Site

We used a subset of a larger intensive culture study of loblolly pine and sweetgum (*Liquidambar styraciflua* L.) owned and managed by International Paper Corporation. The site is located in Decatur County, Georgia, about 16 km southwest of Bainbridge. We worked exclusively in 5-yr-old loblolly pine plots with 2.4 by 3.7 m tree spacing. The study has a randomized complete block design with three blocks and four treatments. Treatments include control (weed control only), irrigation (drip irrigation and weed control), fertigation (drip irrigation with a fertilizer solution and weed control), and fertigation and pest control (drip irrigation with fertilizer solution, weed control, and pest control). Samuelson (1998) describes the site and cultural treatments in greater detail. The site is located in a nearly level area of Troup and Lucy soils. The deep, somewhat excessively drained Troup soil and the very deep, well-drained Lucy soil formed in sandy and loamy marine and fluvial sediments of the Southern Coastal Plain. Troup soil is a member of the loamy, kaolinitic, thermic Grossarenic Kandiudults family. Lucy soil is a member of the loamy, kaolinitic, thermic Arenic Kandiudults family. These soils contain <10% (by volume) rounded quartz gravel, ironstone nodules, and plinthite.

Radar Equipment

The Subsurface Interface Radar (SIR) System-2000, manufactured by Geophysical Survey Systems, Inc. (North Salem, NH) was used in this study. The SIR System-2000 consists of a digital control unit (DC-2000) with keypad, LCD VGA screen, and connector panel. We used a model 5100 (1.5 GHz) antenna(Geophysical Survey Systems, Inc., North Salem, NH), which has a bow tie, dipole configuration. A 12-V DC battery powers the system.

Ground-penetrating radar is a time-scaled system. This system measures the time that it takes electromagnetic energy to travel from the antenna to an interface (e.g., root, soil horizon, stratigraphic layer) and back. To convert the travel time into a depth scale, either the velocity of pulse propagation or the depth to a reflector must be known. The relationships among depth (D), two-way pulse travel time (T), and propagation velocity (V) are described in the following equation (after Morey, 1974):

$$D = V \times T/2$$

Velocity is expressed in meters per nanosecond (m ns^{-1}). The amount and physical state (temperature dependent) of water have the greatest effect on the velocity of propagation. The radar unit was calibrated before fieldwork. A velocity of propagation for the upper part of the soil profile was estimated by burying a metallic object at a depth of 35 cm. Based on the round-trip travel time to the buried reflector, the average velocity of propagation was estimated to be 0.1355 m ns^{-1}. It was not necessary to perform any adjustment to the surface pulse. With the 1.5-GHz antenna, the position of the surface pulse did not significantly affect depth measurements. Based on a velocity of propagation of 0.1355 m ns^{-1}, a scanning time of 10 ns provided a maximum penetration depth of approximately 70 cm at our study site. Once the SIR-2000 settings were optimized for this site, all data were collected with identical parameters (Table 1).

Table 1. Control settings used on SIR-2000 unit.

Parameter	Value
Sample/scan	256
Bits/sample	16
Scans/second	46
Stacking	0
Units	N
Scan unit	200
Unit mark	0
Dielectric constant	4.9
Position	187.9
Range	10†
GAIN	0 16 30 40
Low pass filter	4016
High pass filter	251
Horizontal smoothing	3

† nanoseconds.

Field Procedures

All field activities were completed 11 Dec. through 13 Dec. 2000. There was no significant precipitation during the sampling period; skies were overcast with persistent fog during the day. In treatments receiving irrigation or fertilization, drip irrigation lines were located immediately adjacent to the trees in each row. Within each block, one transect 3.6 m long was established in each treatment. The transect was equidistant between trees and perpendicular to rows in a linear fashion (Fig. 1). Seven sample points were located every 60 cm along each transect line and marked by thin wooden rods that would not produce signal interference. A pass with the 1.5-GHz antenna was made in one direction keeping a steady rate of advance. The location of each sample point was electronically marked on the radar profile as the antenna was pulled passed each wooden rod. A second pass was made in the opposite direction on the other side of the line of rods. Once GPR sampling was complete, a 15-cm soil core was collected to a depth of 30-cm at each sample point. The roots were separated from soil using a standard #14 mesh sieve and washed with water. They were separated into three size classes (0–2, 2–5, and >5 mm), oven-dried at 65°C for 72 h and weighed to determine total live root biomass. Butnor et al. (2001) were unable to satisfactorily separate root size classes or even depth classes of root biomass in shallow profiles. Orientation of roots, geometry of root reflective surfaces and proximity of other adjacent roots all serve to confound attempts to delineate root size classes with GPR. Clusters of small roots can create a point reflector indistinguishable from one larger root. For these reasons only total live root biomass for the entire 0- to 30-cm profile was analyzed in this investigation.

Post-Collection Data Processing

Radar profile normalization and post-collection filtration was accomplished using Radan for Windows NT post-pro-

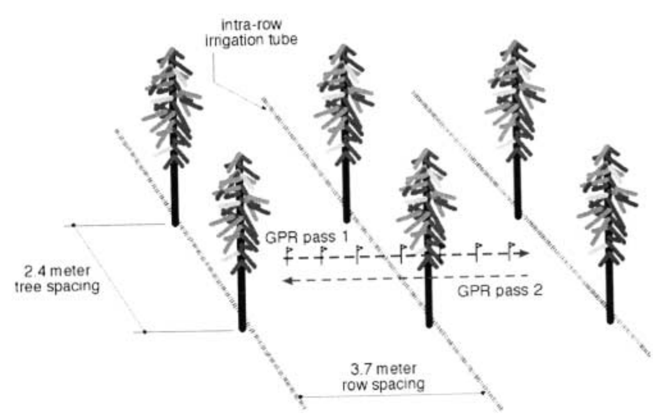

Fig. 1. Illustration of study site showing the location and orientation of trees, irrigation tubes, transects, and GPR passes.

cessing software Version 3.0 (Geophysical Survey Systems Inc., North Salem, NH). Horizontal distance normalization was applied to all profiles to standardize the distance between the markers (rods spaced on the ground at intervals of 60 cm). We did not have a standard distance measured before the first sample point and after the last sample point to properly normalize Cores 1 and 7 (location 0 and 360 cm on the transect). Therefore only the middle five cores of each transect could be analyzed.

After this process, all data files were the same length. Several data processing techniques were applied in a stepwise fashion to determine if they aided in root biomass discrimination. The features of interest in the radar profiles were hyperbolic reflectors that indicate a root or other point anomaly. Parallel bands observed in the scans were the result of plane reflectors such as the ground surface, soil horizons, and bands of low frequency noise. They were removed using a filtration technique called background removal (Oppenheim and Schafer, 1975). Kirchoff migration is a technique that identifies the geometry of a hyperbolic reflector and reduces the impact of multiple reflections (Oppenheim and Schafer, 1975; Berkhout, 1981; Daniels, 1996). This migration technique decomposes and compacts the geometry of the hyperbolas into a form that is closer to the actual feature. The Hilbert transformation is a technique with similar goals as Kirchoff migration, but instead of using geometry, it uses magnitude to decompose the hyperbolic reflectors and multiple "echoes" (Oppenheim and Schafer, 1975). Both of these techniques reduce clutter and help resolve root materials. After these processing techniques were applied separately, the profiles were converted from radar data files (*.dzt) to bitmap image files (*.bmp) using Radan to Bitmap Conversion Utility version 1.4 (GSSI, North Salem, NH).

Quantification of radar profiles was performed with SigmaScan Pro Image Analysis software, Version 5.0 (SPSS Science, Chicago, IL). Radar profiles were converted to 8-bit gray scale images (required by SigmaScan Pro). To make a direct comparison with root biomass collected with soil cores, radar profiles were sectioned with SigmaScan Pro, leaving only the data collected when the antenna was directly over the location of each soil core. Ground-penetrating radar data that could not be directed correlated with cores was discarded. The remaining sections were analyzed with SigmaScan Pro to quantify the relative proportion of the images that presented tree roots as measured by pixel intensity. Intensity is a relative measure of how light or dark a pixel is, using 8-bit grayscale images, a value of 0 is black and 255 is white. We used an intensity threshold range of 60 to 200, which seemed to delineate detectable roots (>0.5 cm) with minimum illumination of unwanted clutter. This thresholding technique illuminates the area of the radar profile that meets the intensity parameters measured by the software. For each transect, data from the two radar passes were used. The area within the intensity threshold parameters for the two passes was combined for each core.

Statistical Analysis

All statistical analyses were performed with the SAS System for Windows Version 8.0 (SAS Institute, Cary, NC). Pearson's correlation coefficient was used to compare actual root biomass from soil cores to radar data, and assess the utility of several signal-processing techniques. Analysis of covariance was used to identify differences in slopes between treatments and provide a linear fertilizer correction equation. Linear regression was used to test these corrections. Analysis of variance using a split-plot design was applied to gauge the impact of block, treatments and core locations on actual and estimated root biomass. Sample means and standard errors presented in bar graphs were calculated with the means procedure.

RESULTS

Images representative of a low root biomass (control) and high root biomass radar profiles (irrigated) are presented in Fig. 2. The midpoint of each image is the location of the center of the tree row, tapering at either end to the inter-row area. Arrows indicate the location of each soil core along the transect. Figure 2A shows a data file that has been horizontally normalized. The control has a smaller number of point reflectors and overall smaller area of high amplitude signal. Another feature to note is the presence of parallel bands from the air-soil interface. These bands do not provide any information on point reflectors and were removed in Fig. 2B using the background removal technique. Kirchoff migration is applied to the data in Fig. 2C. The hyperbolic point reflectors are decomposed into a smaller area, reducing clutter and allowing more precise delineation of objects. Application of the Hilbert transformation is displayed in Fig. 2D. The Hilbert transform and Kirchoff migration technique produce very similar graphical data.

The majority of the roots collected from soil cores were in the >5-mm size class. These coarse roots comprised 87% of total root biomass on a dry weight basis. A direct comparison was made between total root biomass (0- to 30-cm depth) collected from each core and radar data filtered with each of the signal processing techniques. All of the techniques had significant correlations with actual root biomass (Table 2). The Hilbert transformation had the highest correlation (Table 2). The relationship between actual root biomass from cores and GPR data processed with horizontal distance normalization, background removal, Hilbert transformation, and quantified with intensity thresholding procedures was analyzed with the General Linear Models procedure (Proc GLM, SAS Institute) using treatment as a covariant. The results of the analysis for (i) no separation between treatments, (ii) separation into four treatments, and (iii) separation into two primary treatments (fertilized and unfertilized) are displayed in Fig. 3. The amount of variation explained by the model increases substantially when all four treatments are used as a covariant compared with the analysis using no separation between treatments. There was no significant difference in slopes or y intercepts among fertilized treatments (fertigated and fertigated + pest control) or among unfertilized treatments (control and irrigated). The difference in slopes can best be described in a two-treatment model Fig. 3C. Both slopes ($p = 0.0001$) and intercepts ($p = 0.0015$) are significantly different between the treatments. Based on the relationships in Fig. 3C, the Hilbert transformed GPR data was converted to root biomass using the following equations:

$$\text{Fertilized treatment root biomass} = 1.41 + \text{GPR data} \times 0.009294 \quad [1]$$

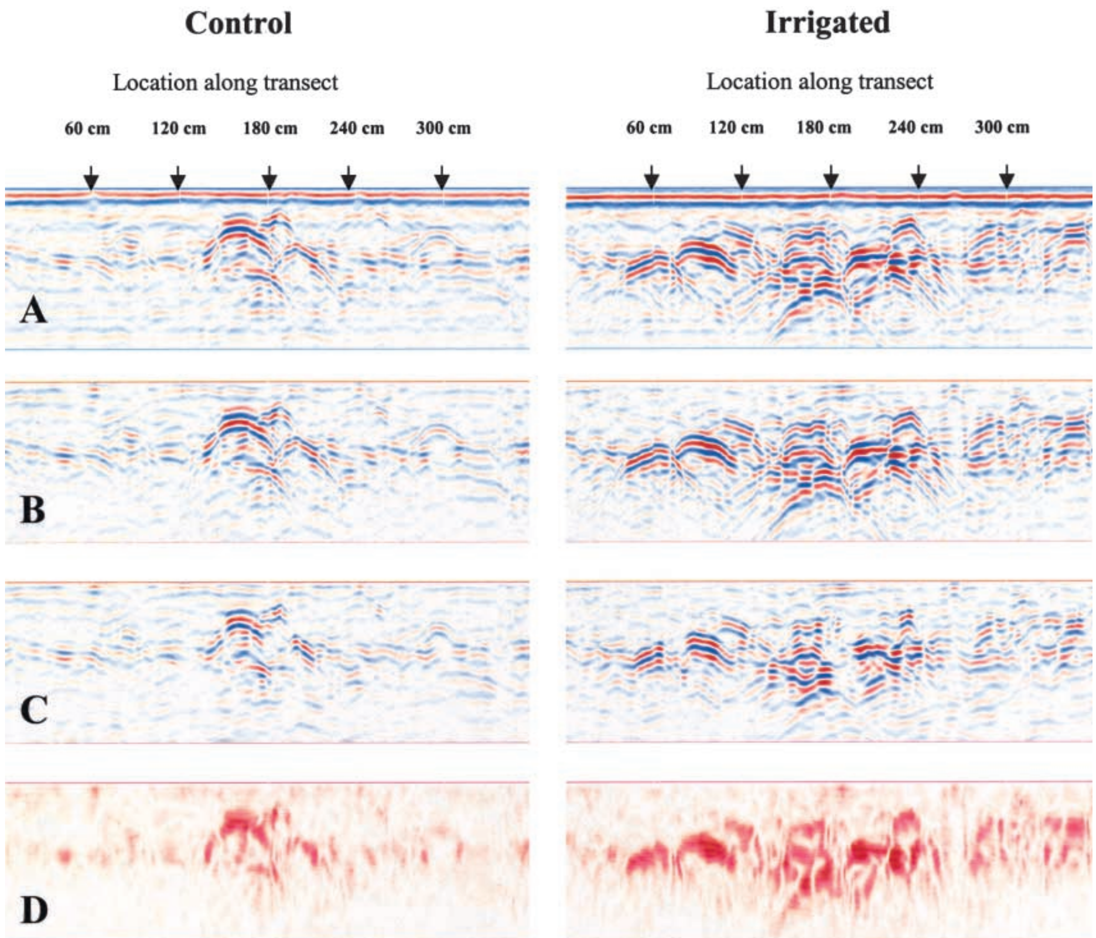

Fig. 2. Radar profiles representative of a low root biomass transect (control) and a high root biomass transect (irrigated). The midpoint of each image is the location of the row center, tapering at either end to the inter-row area. Effect of each digital signal processing procedure on the profile is presented: (A) horizontal distance normalization only, (B) horizontal distance normalization, and background removal, (C) horizontal distance normalization, background removal, and Kirchoff migration, (D) horizontal distance normalization, background removal, and Hilbert transformation.

$$\text{Unfertilized treatment root biomass} = 3.9 + \text{GPR data} \times 0.004834 \quad [2]$$

Once the corrections were applied, linear regression was used to test the relationship between actual root biomass from soil cores and estimated root biomass using GPR. The fertilizer corrections increased the amount of variation explained ($R^2 = 0.73$) and gave a 1:1 ratio between actual and estimated root biomass (Fig. 4). The correlation coefficient between actual root biomass in soil cores and Hilbert transformed GPR data, with the above corrections, improved to $r = 0.86$ ($n = 60$, $p < 0.0001$).

There were no significant differences between actual or estimated root biomass per transect (sum of five cores) by block or treatment (Fig. 5 and 6). Within each treatment the agreement between actual and estimated biomass was very close (Fig. 6). Estimated biomass generally had lower variability than actual biomass harvested from cores.

Table 2. Comparison of root biomass separated from 10 by 30 cm soil cores to radar estimates using Pearson's Correlation Coefficient ($N = 60$).

Processing procedure	r	p
Horizontal distance normalization and background removal	0.73	$<$0.0001
Horizontal distance normalization, background removal and Kirchoff migration	0.81	$<$0.0001
Horizontal distance normalization, background removal and Hilbert transformation	0.76	$<$0.0001

Analysis of variance was utilized to assess the impact of block, treatments, and core locations on actual and estimated root biomass using a split plot design (Tables 3 and 4). Due to greater variability in actual root biomass, the treatments and the treatment/core–location interaction were not found to be significant using a five core per treatment/block combination sampling scheme (Table 3). However, core location was highly significant. Due to less variability in estimated biomass, the treatment, location and treatment/core location interaction were all significant (Table 4). Most of the variability in both actual ($R^2 = 0.81$) and estimated ($R^2 = 0.89$) root biomass was explained by the statistical model. Both ANOVA tables indicate that location along the transect has the greatest impact on root biomass. Data summarized from all three blocks showing root biomass distribution per treatment is presented in Fig. 7. Even though the

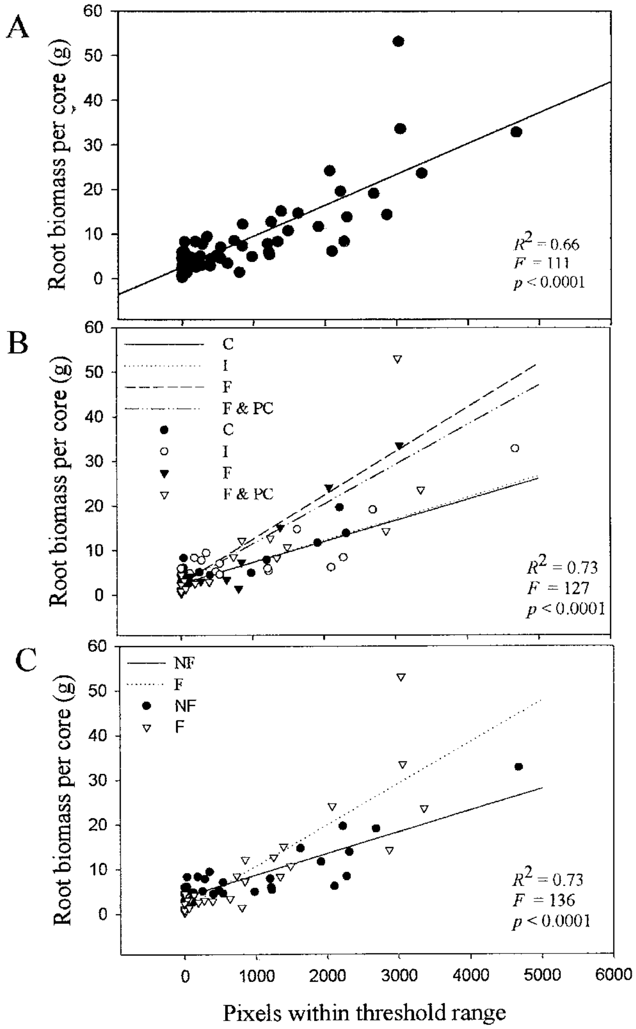

Fig. 3. Relationship between actual root biomass from soil cores and GPR data processed with horizontal distance normalization, background removal, Hilbert transformation, and thresholding procedures. Analysis of covariance results using (A) no treatment delineation, (B) separation in four treatments, and (C) reduction to two primary treatments.

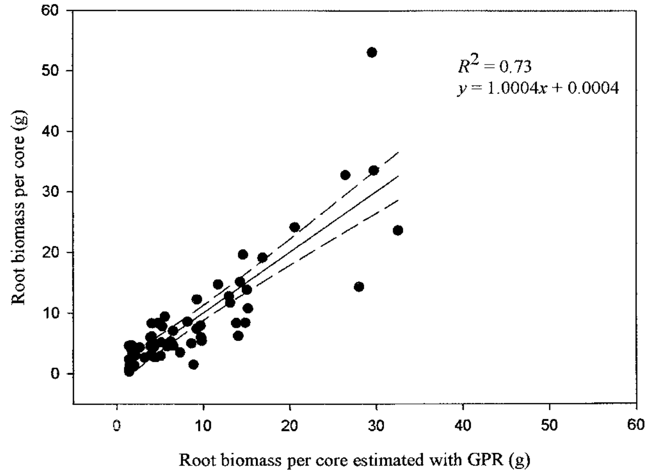

Fig. 4. Linear regression comparing total root biomass per core and root biomass estimated with GPR, which has been adjusted to account for fertilizer effects on signal magnitude. Dashed lines represent the 95% confidence interval.

control treatment has no drip irrigation tube, root biomass is greater on the row center, which is closer to the trees than any other core location. The other treatments that receive irrigation and/or fertilization have dramatically higher root biomass near the drip tube (Fig. 7.). Excellent agreement exists between actual and estimated root biomass, with estimated biomass exhibiting similar or lower variation as gauged by the standard error of the mean.

DISCUSSION

Substantial improvement of root biomass estimation with GPR was possible with the aid of advanced digital signal processing techniques. Horizontal distance normalization and background removal techniques are necessary to standardize data sets. Background removal eliminated obvious clutter from surface reflections and undesired, low-frequency background noise consisting of parallel reflections in the data (Fig. 1). Kirchoff curve migration improved the correlation between actual and estimated root biomass (Table 2), but not as much as the Hilbert transformation. With the Radan for Windows NT program, the user defines the hyperbola and then only one definition of hyperbola geometry is used to analyze point reflectors in the data set and remove clutter. Unlike civil engineering targets (rebar, buried pipes, construction material layers) tree roots have a tremendous diversity of reflector shapes and orientations. The one size fits all geometry definitions utilized in curve migration (as performed in this study) is not as useful as the Hilbert transformation. The Hilbert transform uses signal magnitude instead of reflector geometry to compact the hyperbola into a shape more representative of the actual size of the point anomaly. No user-defined parameters are necessary to run the Hilbert transform, eliminating the need for potentially arbitrary decisions on hyperbola geometry.

In this study we found that fertilizer applications had a significant effect on the amplitudes of the reflected radar signal. A larger quantity of root biomass in the fertilized treatment produces lower signal amplitudes than a smaller quantity of roots in the unfertilized treatments (Fig. 3). We were able to statistically correct the data to account for these effects (Eq. [1] and [2]) and improve correlations between actual and estimated root biomass (Table 2). Increased soluble salt contents will increase the electrical conductivity and the attenuation rate of radar energy in soils. The greater dissipation of radar energy in the fertilized treatment plots results in lower amplitude reflections. Ions resulting from fertilizer application may cause increased electrical conductivity at the soil-root interface thereby reducing the size and magnitude of the resulting hyperbola relative to a point anomaly without fertilizer. Calibration of radar by treatment solves the problem of treatment bias on radar signal propagation. This finding may have implications for how GPR data is used quantitatively in fertilized agricultural systems.

This research substantially improved root biomass

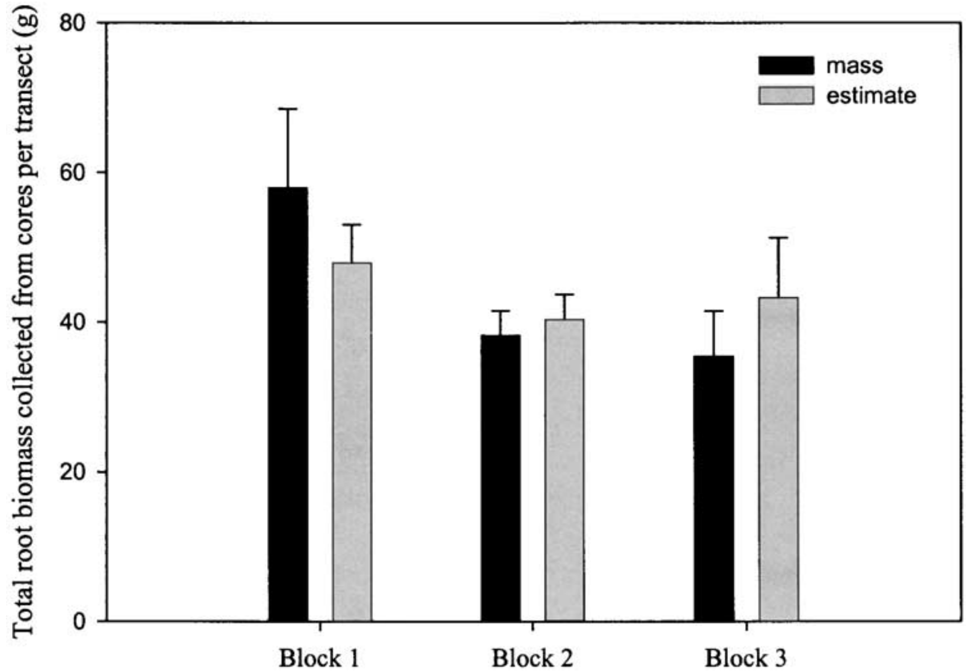

Fig. 5. Comparison of total root biomass per transect (five cores) and root biomass estimated with GPR (adjusted to account for fertilizer effects on signal magnitude) within each block (+/− s.e.).

estimation over previous studies (Butnor et al., 2001) by closely matching the footprint of the radar antenna to the location of the soil core. The ability to correlate radar data to actual root biomass ($r = 0.86$) gives greater confidence in the technique. Root biomass estimates from cores can be highly variable where root distribution is uneven. The quality of these estimates is dependent on matching sample size and coefficient of variation. Retzlaff and others (2001) present data comparing lateral root density (non-taproot) in a 5 yr-old loblolly pine plantation measured with 1-m^2 pits ($n = 3$ per plot) and estimated with 5-cm soil cores ($n = 6$ [four pooled subsets per n] per plot). Lateral root density from the squared-meter pits was 60% higher than core estimates with a range of −9 to 143%. Vogt and Persson (1991) found that soil cores were useful to study fine roots (<2 mm), but unsuited to estimate coarse roots because of the unequal distribution and decreasing density as distance from the taproot grows. Previous studies indicated that roots as small as 5 mm are directly detectable with GPR (Butnor et al., 2001). In the current study 87% (dry weight basis) of roots were directly detectable with GPR. This is not to imply that roots <5 mm were not measured, but they could not be resolved singly. Problems encountered estimating root biomass with soil cores can be greatly minimized by the quantity of data obtained with GPR. Once a research site is calibrated for root studies with soil cores, the potential to study root biomass distribution with GPR is remarkable (Fig. 7). In each transect a linear distance of 3.6 m was scanned. However, data were only used where we had direct verification with soil cores (five per transect). Each transect took minutes to scan and contains data equivalent to 36 cores. An additional 1000 m was scanned at the site in <4 h, yielding data equivalent to 10 000 soil cores (data not shown). The effort of coring a small subset of a forest research site can be leveraged with GPR, yielding vast quantities of data. Future research will address scaling to the stand level and developing root biomass distribution contour maps for different cultural treatments.

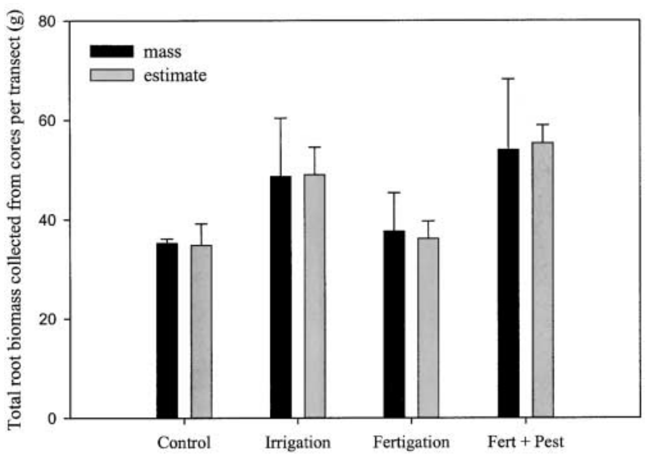

Fig. 6. Comparison of total root biomass per transect (five cores) and root biomass estimated with GPR (adjusted to account for fertilizer effects on signal magnitude) within each treatment (+/− s.e.).

Table 3. Analysis of variance table for actual root biomass collected via soil cores in the replicated experiment ($R^2 = 0.81$).

Source	df	SS	MS	F	p
Block	2	241.49			
Treat	3	142.19	47.40	1.19	0.3885
Block × Treat (Error A)	6	238.04	39.67		
Location	4	2875.58	718.90	23.23	0.0001
Treat × Location	12	485.16	40.43	1.31	0.2626
Block × Location + Block × Location × Treat (Error B)	32	990.12	30.94		

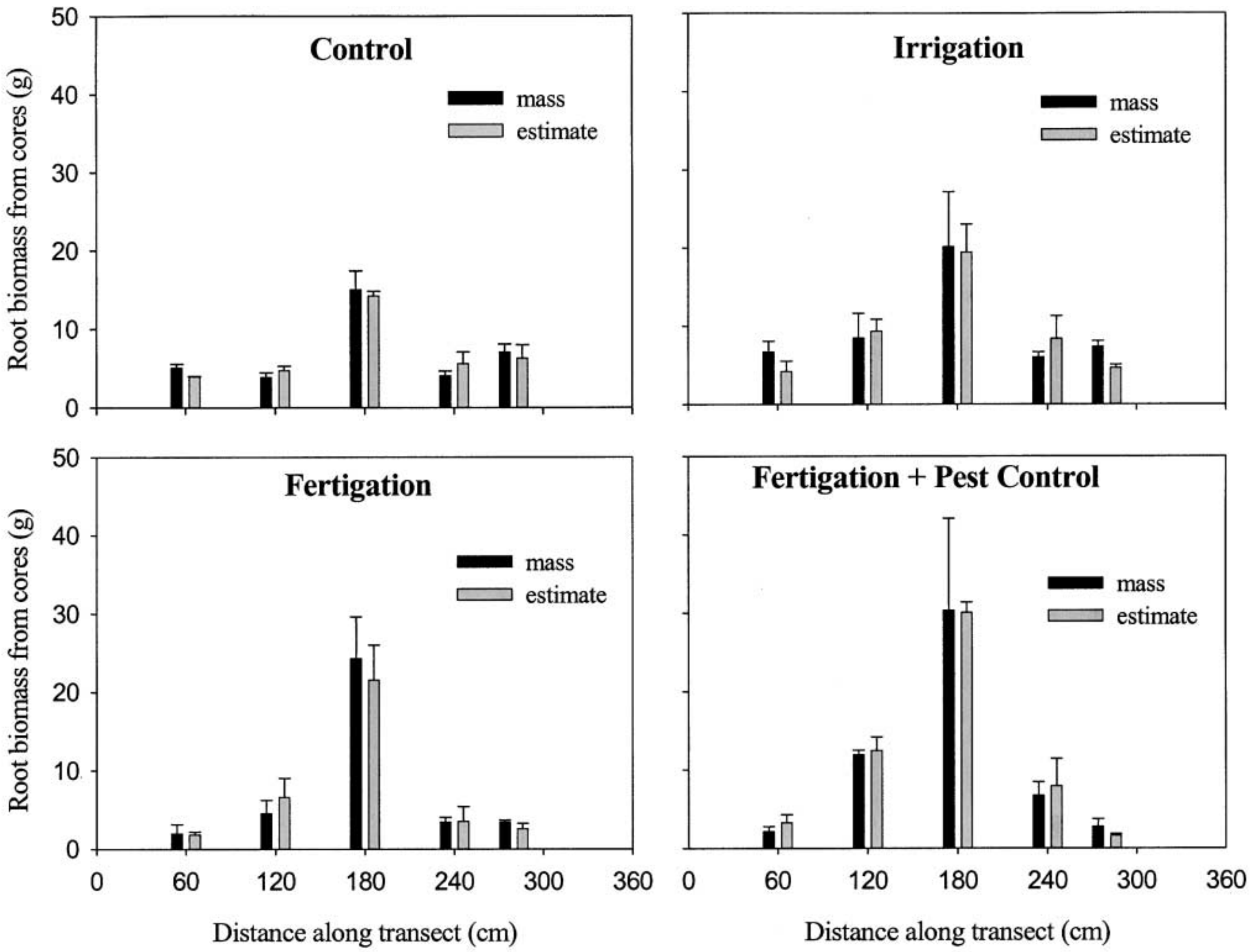

Fig. 7. Effect of soil core location along the survey transect on root biomass (actual and estimated in each treatment (+/− s.e.). Except for the control treatment, drip irrigation/fertigation tubes cross the transect at 180 cm.

If actual and radar estimates of root biomass have a high correlation ($r = 0.86$) we would expect that when analysis of variance is applied to both sets of variables they would have similar results. Estimated biomass was able to detect levels of significance in treatment and treatment/core location that were not possible with the soil core data (Table 3 and 4). Apparently the amount of variability among soil cores is greater than that estimated with GPR. Although we marked the exact location of the soil core on the GPR data, we had limited control over the exact size of the antenna's footprint area. Conyers and Goodman (1997) describe factors that influence the footprint area. We likely measured an area somewhat larger than the soil core and small point-to-point heterogeneity present in the cores was reduced.

Table 4. Analysis of variance table for estimated root biomass, using soil core calibrated radar data, in the replicated experiment ($R^2 = 0.89$).

Source	df	SS	MS	F	p
Block	**2**	**23.67**			
Treat	**3**	**179.06**	**59.69**	**5.56**	**0.0363**
Block × Treat (Error A)	**6**	**64.46**	**10.74**		
Location	**4**	**2528.6**	**632.15**	**51.59**	**0.0001**
Treat × Location	**12**	**444.64**	**37.05**	**3.02**	**0.0061**
Block × Location + Block × Location × Treat (Error B)	**32**	**392.13**	**12.25**	**51.59**	**0.0001**

Ground-penetrating radar provides better root biomass distribution data than coring alone, but neither technique can adequately measure taproot biomass. The importance of the taproot and stand level measurements is dramatic (Table 5). Taproots comprised 50 to 94% of the total root biomass in several loblolly pine plantations measured in the southeastern USA (Table 5). More work is needed to develop non-invasive methodologies to measure this component of root biomass. Unlike lateral roots, we do not need to search for taproots, we know their location and should be able to angle the GPR antenna or use borehole methods to image the taproot. It should also be noted that taproot biomass can be estimated very successfully with allometric equations designed for specific site conditions (Albaugh et al., 1998). However, this is a time consuming and expensive process.

Our study site was, a priori, considered to be amenable to radar investigation. When considering GPR for use in forest research, careful attention to soil suitability (Doolittle et al., 2002) and other site factors that can

Table 5. Mean percentage of total root biomass comprised of a vertically oriented taproot in loblolly pine plantations receiving varied cultural treatments and nutrient amendments.

Stand age	Taproot†	Location	Reference
yr			
5	94	Decatur County, GA	Samuelson, unpublished data (2001)
5	>50	Scotland County, NC	Retzlaff et al. (2001)
15	82	Scotland County, NC	T.J. Albaugh, personal communication (2001)
34	63	Union County, SC	Richter et al. (1995)
55	55	Oconee County, SC	Van Lear et al. (1995)

† Percentage of total root biomass comprised of taproot.

limit resolution of tree roots (Butnor et al., 2001) is necessary. The type of antenna used in this study requires contact with the soil surface. It needs to be advanced (pulled) across the surface at a controlled pace with minimal tipping or bouncing as the antenna moves over small obstacles. Complete weed control was practiced at this research site, effectively eliminating understory vegetation. The antenna could glide easily over pine litter, but any large woody debris were moved from the transect. The presence of undergrowth, raised beds, logs, or logging slash will limit the utility of GPR to delineate tree roots (Butnor et al., 2001) and require additional site preparation before GPR surveys can be conducted.

Ground-penetrating radar can be used to determine soil moisture (Dubois et al., 1995; Chanzy et al., 1996). The impact of variations in soil moisture on root biomass calibrations over the course of seasons or years is unknown. Since our study was performed over a short period of time without appreciable changes in soil moisture content, any potential differences in soil moisture would be accounted for by the destructive sampling of the soil cores. The fact that irrigated and control treatments had nearly identical slopes when comparing actual and estimated root biomass (Fig. 3B) indicates that any potential soil moisture differences did not significantly impact GPR during this study. Additional research integrating root biomass and soil water content estimation is necessary before GPR is used for repeated root biomass surveys over seasons or years or more topographically diverse sites.

CONCLUSIONS

We found that GPR can be used to augment root biomass surveys. The utility of GPR is greatly increased using a Hilbert signal transformation approach. Following signal processing, correlations between root coring and GPR exceed 85%. Some of the residual variability appears to be a result of difficulty with core sampling and may not be easily improved upon solely by improved GPR technique. Differences in fertilization and, perhaps other silvicultural treatments affect the GPR signals. Although corrections for such treatments differences can be made, this suggests that it is unlikely that universal calibration can be utilized in experimental research even when species and soil conditions are held constant. In compatible soils, the use of GPR can drastically reduce the number of soil cores that are needed to assess tree root biomass and biomass distribution. The quality and quantity of information resulting from a detailed GPR survey can rapidly estimate root biomass and provide unparalleled information on lateral root biomass distribution and quantity.

ACKNOWLEDGMENTS

We thank Dan Delea and Geophysical Survey Systems, Inc., for technical assistance and the use of the 1.5-GHz antenna, their support and advice was essential to this project. We appreciate the access provided by International Paper Corporation to their field site. Rodney Kindlund assisted with the preparation of figures.

REFERENCES

Albaugh, T.J., H.L. Allen, P.M. Dougherty, L.W. Kress, and J.S. King. 1998. Leaf area and above- and below-ground growth responses of loblolly pine to nutrient and water additions. For. Sci. 44:1–12.

Berkhout, A.J. 1981. Wave field extrapolation techniques in seismic migration, a tutorial. Geophysics 46:1638–1656.

Butnor, J.R., J.A. Doolittle, L. Kress, S. Cohen, and K.H. Johnsen. 2001. Use of ground-penetrating radar to study tree roots in the southeastern United States. Tree Physiol. 21:1269–1278.

Chanzy, A., A. Tarussov, A. Judge, and F. Bonn. 1996. Soil water content determination using a digital ground-penetrating radar. Soil Sci. Soc. Am. J. 60:1318–1326.

Conyers, L.B., and D. Goodman. 1997. Ground-penetrating radar: An introduction for archaeologists. Alta Mira Press, Walnut Creek, CA.

Daniels, D.J. 1996. Surface-Penetrating Radar. The Institute of Electrical Engineers, London, U.K.

Doolittle, J.A., F.E. Minzenmayer, S.W. Waltman, and E.C. Benham. 2002. Ground-penetrating radar soil suitability map of the conterminous United States *In* S. Koppenjan and H. Lee (ed.) 9th International Conference on Ground Penetrating Radar, Santa Barbara, CA, 29 Apr.–2 May 2002, Proceedings of SPIE—The International Society of Optical Engineering, Bellingham, WA. 4758:7–12.

Dubois, P., J. Van Zyl, and T. Engman. 1995. Measuring soil moisture with imaging radars. IEEE Trans. Geosci. Remote Sens. 33:915–926.

Morey, R.M. 1974. Continuous subsurface profiling by impulse radar. p. 212–232. *In* Proceedings, ASCE Engineering Foundation Conference on Subsurface Exploration for Underground Excavations and Heavy Construction, 11–16 Aug. 1974. Henniker, N.H.

Oppenheim, A.V., and R.W. Schafer. 1975. Digital Signal Processing. Prentice Hall, Inc. Englewood Cliffs, NJ.

Retzlaff, W.A., J.A. Handest, D.M. O'Malley, S.E. McKeand, and M.A. Topa. 2001. Whole-tree biomass and carbon allocation of juvenile trees of loblolly pine (*Pinus taeda*): Influence of genetics and fertilization. Can. J. For. Res. 31:960–970.

Richter, D.D., D. Markewitz, J.K. Dunsomb, P.R. Heine, C.G. Wells, A. Stuanes, H.L. Allen, B. Urrego, K. Harrison, and G. Bonani. 1995. Carbon cycling in a loblolly pine forest: Implications for the missing carbon sink and for the concept of soil. p. 233–251. *In* W.W. McFee and J.M. Kelly (ed.) Carbon forms and functions in forest soils. SSSA, Madison, WI.

Richter, D.D., D. Markewitz, S.E. Trumbore, and C.G. Wells. 1999. Rapid accumulation and turnover of soil carbon in a re-establishing forest. Nature 400:56–58.

Samuelson, L.J. 1998. Influence of intensive culture on leaf net photosynthesis and growth of sweetgum and loblolly pine seedlings. For. Sci. 44:300–316.

Van Lear, D.H., P.R. Kapeluck, and M.M. Parker. 1995. Distribution of carbon in a Piedmont soil as affected by loblolly pine management. p. 489–501. *In* W.W. McFee and J.M. Kelly (ed.) Carbon forms and functions in forest soils. SSSA, Madison, WI.

Vogt, K.A., and H. Persson. 1991. Measuring growth and development of roots. p. 477–501. *In* J.P. Lussoie and T.M. Hinckley (ed.) Techniques and approaches in forest tree physiology. CRC Press, Boca Raton, FL.

Wielopolski, L., G. Hendrey, and M. McGuigan. 2000. Imaging tree root systems *in situ*. *In* D.A. Noon, G.F. Stickley, and D. Longstaff (ed.) Proceedings of the 8th International Conference on Ground-Penetrating radar, Gold Coast, Queensland, Australia, 23–26 May 2000. Proceedings of SPIE—The International Society of Optical Engineering, Bellingham, WA. 4084:642–646.